This article has been accepted for publication in a future issue of this journal, but has not been fully edited. Content may change prior to final publication. Citation information: DOI 10.1109/JLT.2016.2521173, Journal of Lightwave Technology

Brillouin Optical Correlation Domain Analysis Addressing 440,000 Resolution Points

Yosef London, Yair Antman, Eyal Preter, Nadav Levanon, and Avi Zadok

***Abstract*— The distributed Brillouin analysis of an 8.8 km long fiber with a spatial resolution of 2 cm is presented. All 440,000 potential resolution points are addressed in the measurement. A 7 cm-long hot-spot, located towards the output end of the pump wave, is properly identified in the experiment. The experimental error in the estimate of the local values of the Brillouin frequency shift is ±3.5 MHz. The analysis is based on the simultaneous generation and analysis of Brillouin interaction in more than 2,000 correlation peaks, induced by periodic phase modulation of the pump and signal waves. The Brillouin amplifications at individual peaks are resolved using radar-like coding of pump wave magnitude by a 10,000 bit-long aperiodic sequence, and post-detection compression at the receiver end. Extensive numerical simulations of the Brillouin interactions over kilometers of fiber with centimeter resolution are reported as well. The results are at the state of the art for high-resolution distributed Brillouin sensors.**

***Index Terms*—Fiber-optic sensors, stimulated Brillouin scattering, all-optical signal processing, sequence compression, distributed fiber sensors, correlation-domain analysis.**

I. Introduction

Stimulated Brillouin scattering (SBS) is a nonlinear interaction between two optical waves, a pump and a frequency-detuned signal, which is mediated by a stimulated acoustic wave [1]. Distributed sensors along optical fibers represent the primary technological application of SBS to-date. Sensor systems rely on the mapping of the local value of the Brillouin frequency shift along a fiber under test, and on the variations of that value with both temperature and mechanical strain [2, 3]. The measurement principles were first proposed 25 years ago [2]. Readily available commercial sensor systems provide a measurement range of tens of kilometers, sub-meter spatial resolution and sensitivity on the order of 1 °C or 20 με, with acquisition times of minutes. These systems are employed in the monitoring and protection of critical, large-scale infrastructures, primarily in the energy and oil-and-gas sectors.

Manuscript received October 22nd, 2015; revised January 20th, 2016; accepted January 21st, 2016. This work was supported in part by the Chief Scientist Office of the Israeli Ministry of Economy, through the KAMIN and MAGNETON programs.

Yosef London, Yair Antman, Eyal Preter and Avi Zadok are with the Faculty of Engineering, Bar-Ilan University, Ramat-Gan 5290002 Israel. (Email: Avinoam.Zadook@biu.ac.il).

Nadav Levanon is with the School of Electrical Engineering, Faculty of Engineering, Tel-Aviv University, Ramat-Aviv, Tel-Aviv 6997801, Israel. (Email: nadav@eng.tau.ac.il)

In recent years, rapid and significant advances in performance of SBS-based sensors have been reported in the literature. The range of measurement was extended to a 600 km-long fiber loop, using distributed Raman amplification and cascaded, inline erbium-doped fiber amplifiers (EDFAs) [4]. Dynamic measurement capabilities, reaching kHz rates over more than a hundred meters, have supported the distributed Brillouin analysis of structural vibrations [5-9]. Last but not least, spatial resolution has been improved towards the cm- and even mm-scale. High resolution capabilities open up significant new areas of application for SBS sensors, in the civil engineering, aerospace, transportation and medical sectors. Much effort is being dedicated by the fiber-sensors research community to extend the range and the number of addressed points in high-resolution Brillouin analysis.

In this work, we report the experimental Brillouin analysis of an 8.8 km-long fiber with a spatial resolution of 2 cm. The entire set of 440,000 resolution points was successfully analyzed. Compared with our previous work [10], the number of points has increased four-fold. To the best of our knowledge, the results represent the largest set of resolution points addressed by an SBS-based sensor. A 7 cm-wide local hot-spot, located towards the output end of the pump wave, was successfully identified in the measurements. The experimental error in the estimate of the local Brillouin frequency shift was ±3.5 MHz, corresponding to an uncertainty of ±3.5 °C or ±70 με.

The measurement protocol is based on the simultaneous generation and analysis of SBS gain in over 2,000 discrete, narrow and controllable locations. The Brillouin interactions are sequence-coded, and resolved using a compression protocol that was inspired by radar principles [11,12]. The suppression of shot and detector noise provided by the analysis of a single sequence is equivalent to that obtained in the averaging of 3,000 single-pulse experiments. The analysis protocol is also investigated in numerical modelling of SBS, carried out for several km of fiber with cm resolution. These extensive simulations of Brillouin sensors are seldom addressed.

The remainder of this paper is organized as follows: Background on high-resolution Brillouin sensors is given in section 2, intended for the non-specialists. The analogy between distributed Brillouin sensors and radar systems, and its implications in sequence coding, are addressed in section 3. Numerical simulations are reported in section 4. Experimental setup and results are presented in section 5. A concluding discussion is provided in section 6. The results were briefly presented in [13].

II. High-resolution distributed Brillouin analysis protocols

The traditional and most widely-employed SBS sensing principle to-date is Brillouin optical time domain analysis, or B-OTDA [2,3]. In B-OTDA systems an intense, comparatively short pump pulse is launched from one end of the fiber, and a weaker, continuous and a frequency-detuned signal is transmitted from the opposite end. The spatial profile of Brillouin amplification is recovered from the analysis of the output signal wave as a function of time. Measurements are repeated for several frequency offsets between pump and signal, until the Brillouin gain spectra along the fiber are reconstructed. Resolution in the fundamental B-OTDA method equals the spatial extent of the pump pulse. The duration of pulses must exceed the lifetime associated with the stimulation of the acoustic wave, which is on the order of 5 ns [1]. Therefore, B-OTDA resolution has been limited to approximately 1 meter [14].

Numerous techniques were proposed to circumvent the acoustic lifetime limitation and extend B-OTDA resolution [15,16]. In pre-excitation-based protocols, an acoustic field is first stimulated by a long pedestal of a comparatively week pump wave [17]. That acoustic field is then probed by an abrupt change in pump power or phase. The measurement resolution is governed by the transition time of the pump, rather than by the acoustic lifetime. Several variants of this concept were successfully demonstrated [18-20]. In double-pulse measurements, the output signal wave is acquired twice, with pump pulse durations that are slightly different, and the two traces are subtracted in post-processing [21]. The obtained resolution is determined by the difference between the durations of the two pulses, and not by their absolute extent. B-OTDA experiments have reached a spatial resolution of 2 cm over 2 km of fiber [22], and 5 cm over a 5 km range [20].

An alternative SBS sensing paradigm relies on manipulating the cross-correlation function between the complex envelopes of the pump and signal waves [23]. The magnitude of the acoustic wave in a given location is closely related to the correlation between the two optical waves at that point. This property is at the basis of Brillouin optical correlation domain analysis (B-OCDA), in which the pump and signal are modulated so that their correlation is restricted to discrete and narrow peaks [23]. The SBS interaction is largely confined to these peaks, where it is stationary [23]. B-OCDA therefore removes the link between temporal duration of pulses and spatial resolution. The analysis of 24,000 high-resolution points [24], and a spatial resolution as high as few mm [25-26], have been achieved.

The range of unambiguous measurements in B-OCDA is limited by the generation of multiple correlation peaks, separated by the modulation period. In 2012, our group together with the Thevenaz group of EPFL proposed a protocol in which the two optical waves were jointly modulated by a high-rate, periodic binary phase sequence, which could be arbitrarily long [27]. Phase-coding effectively decouples between resolution and range of unambiguous measurements in B-OCDA [28].

Despite much progress in recent years, the extension of both high-resolution B-OTDA and B-OCDA towards 100,000 resolution points and beyond faces several challenges. First and foremost, the power gain of the signal over a cm of fiber is extremely weak, on the order of 0.1% for 1 W of pump power. The characterization of such little gain with sufficient fidelity in the presence of noise is difficult, and often mandates averaging over many repeating acquisitions. Pump power in high-resolution B-OTDA is restricted by depletion and by the onset of spontaneous Brillouin scattering. In addition, B-OTDA requires broadband detection, at 10 GHz bandwidth for 1 cm resolution, which increases noise variance. B-OCDA is more immune to depletion and requires much narrower detection bandwidths of tens of MHz, but suffers from interference due to residual off-peak SBS interactions that do not vanish entirely [27]. Furthermore, the scanning of correlation peaks positions over long fibers might require prohibitively long durations.

An important step towards partially resolving these issues was taken in parallel by Denisov et al. [29] and by our group [30], in overlaying an amplitude pulse modulation on top of phase-coded B-OCDA. A short, periodic phase modulation sequence was chosen, so that a large number of correlation peaks could be introduced along the fiber [30]. However, the amplitude pulse modulation guaranteed that only a single correlation peak was established at any given instance. The SBS interactions taking place at the different locations could be resolved in the time domain, much like in a B-OTDA.

The advantage of this hybrid approach is two-fold: First, hundreds of correlation peaks could be addressed in a single time-of-flight (ToF), reducing the acquisition durations accordingly [30]. Second, off-peak interactions were restricted to the spatial extent of the pump pulse, rather than span the entire fiber under test. Using this method, we successfully analyzed a 1.6 km-long fiber with a 2 cm resolution [31]. In other experiments, the potential of reaching over a million points has been demonstrated [32,33]. However, only a subset of these points could actually be analyzed.

In order to take high-resolution Brillouin sensing to the next level, the simultaneous analysis of a larger number of points with a better signal-to-noise ratio (SNR) was necessary. The approach taken to that end is described next.

III. Incoherent pulse compression in Brillouin optical correlation domain analysis

A. The radar analogue and incoherent pulse compression

Several parallels can be drawn between distributed Brillouin sensors and radar systems. Both are required to identify and locate irregular patterns in noisy background and at low SNRs. Evaluation of both systems is based on range, resolution, sensitivity and acquisition durations, and both systems may have to resolve multiple events. The similarity is of course incomplete: Brillouin 'targets' are induced by the measurement procedure itself, and fiber sensors are strictly one-dimensional and do not include the equivalent of angular scanning. Nevertheless, many lessons learned by the radar community

This article has been accepted for publication in a future issue of this journal, but has not been fully edited. Content may change prior to final publication. Citation information: DOI 10.1109/JLT.2016.2521173, Journal of Lightwave Technology

may be carried over to distributed fiber sensors.

The phase-coded B-OCDA setup with a single overlaying pump pulse [29-32], discussed at the end of the previous section, may be regarded as the SBS equivalent of a ToF range-finder measuring a large set of discrete targets. Care must be taken in making this comparison as well, as resolution in the B-OCDA case is governed by the modulation rate of the underlying periodic phase code rather than by the amplitude pulse duration. Yet, both systems are able to separate multiple discrete events directly in the time domain. Much like in ToF radars, the amplitude of a single pulse in B-OCDA is restricted (although the reasons of these limitations obviously differ), leaving the averaging over multiple pulses as the sole avenue towards SNR enhancement.

Alternatively, many radar systems spread the transmission energy over an extended sequence of pulses, followed by the compression of collected echoes by a matched-filtering process [34]: the aperiodic correlation of the received sequence with a replica of itself. The measurement retains the high resolution and high SNR of a single, intense pulse, while alleviating the need for transmitting instantaneous peak power levels. Matched-filtering collapses the entire energy of a sequence to a narrow virtual impulse, whose magnitude represents the strength of the radar reflection event [34].

Most codes, however, exhibit nonzero sidelobes of their aperiodic correlation which do not represent real targets. Correlation sidelobes are typically weak, and may be further reduced by more elaborate, mismatched filtering at the receiver end [34]. Nevertheless the sidelobes induced in the processing of a large number of sequence echoes might add up and interfere with the analysis of true events. The primary metric describing the quality of sequence compression is therefore its peak-to-sidelobe ratio (PSLR), defined as the ratio between the magnitude of the main aperiodic correlation peak and that of the highest residual sidelobe. PSLRs of many carefully-constructed sequences scale with their length.

The implementation of sequence coding in optical setups faces a fundamental difficulty. While most high-PSLR sequences involve the transmission and detection of phase information [34], many optical systems are based on direct detection of intensity only. Phase-coded B-OCDA is no exception, as the monitored quantity is the power of the signal wave. Only few SBS sensors to-date have involved the coherent measurement of phase [7,35]. Fortunately, protocols for the efficient compression of incoherently-detected, aperiodic amplitude codes have been developed [11]. Incoherent compression relies on the transmission of a carefully-constructed binary amplitude sequence, and its aperiodic cross-correlation with a complex-valued reference code that is stored at the receiver [12]. The procedures for deriving the amplitude sequences from known phase codes are detailed elsewhere [12,36]. This principle was successfully employed in laser range-finder experiments [12,36], and in image resolution enhancement [37].

The significance of sidelobe suppression is illustrated in the following example. Figure 1(top) shows the compressed form of 600 equal-magnitude echoes of a 2,224 bit-long code used in our earlier work [10], all overlaid. The delay between successive replicas was chosen as twice the duration of individual pulses. A magnified view in the vicinity of the final compressed replica is shown in figure 1(bottom). The aperiodic cross-correlation with a reference sequence properly recovers the 600 individual events, with good uniformity. However, the compression performance is degraded when the number of echoes is increased to 3,000 (figure 2(top)): 'ghost echoes' appear before the first real event and following the final one, and the magnitudes of the identical replicas following compression appear uneven.

Figure 2(bottom) shows the simulated compression of 3,000 echoes of a longer, 9,785 bit-long code, used in the experiments of the current work. The aperiodic cross-correlation between the longer sequence and its mismatched reference has perfectly zero sidelobes, (at least ideally). The compression of 3,000 replicas of that code shows no magnitude variations or ghost events. Note that the simulations do not take into consideration possible degradations due to imperfect pulse shapes, or additive noise.

Figures 1 and 2 also highlight another advantage of the longer code: the processing gain is increased from a factor of 500 up to over 3,000. This factor suggests that the processing of a single trace would suppress additive detector noise and shot noise in a manner that is equivalent to the averaging of over 3,000 single-pulse acquisition. The potential of sequence coding in Brillouin sensors was already recognized in a series of works by Soto et al., who used amplitude sequence coding to extend the range of long-reach B-OTDA [38-41]. The use

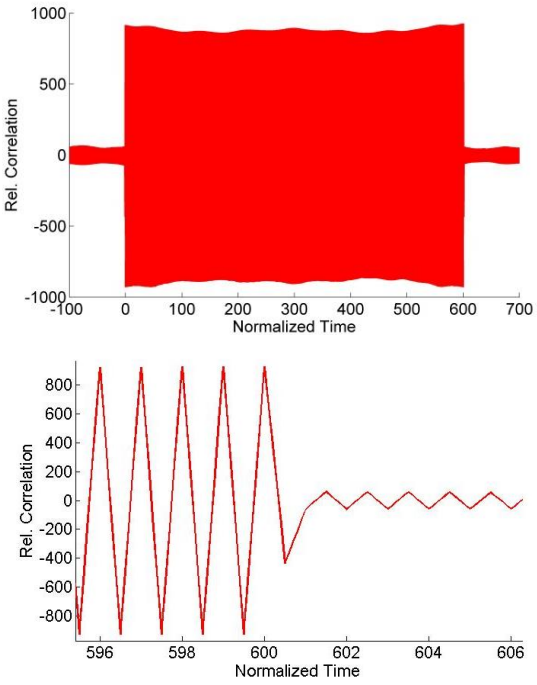

Fig. 1. Top - Compressed form of 600 replicas of a 2,224 bit-long amplitude sequence, used in our previous work [10]. Time axis is normalized to the delay between successive replicas, chosen as twice the duration of individual pulses. The correlation magnitude axis is normalized to the magnitude of individual pulses. Bottom - Magnified view of the compressed trace in the vicinity of the final event.

This article has been accepted for publication in a future issue of this journal, but has not been fully edited. Content may change prior to final publication. Citation information: DOI 10.1109/JLT.2016.2521173, Journal of Lightwave Technology

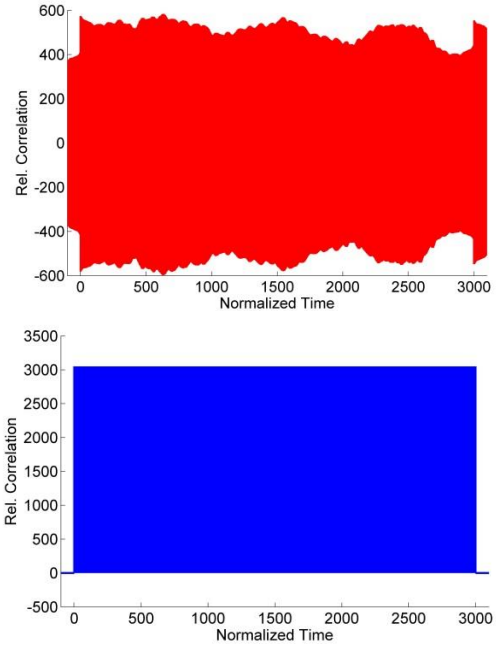

Fig. 2. Top - Compressed form of 3,000 replicas of the code of Fig. 1. Nonzero sidelobes of multiple correlation peaks add up and degrade the compressed trace. Bottom - Compressed form of 3,000 echoes of a 9,785 bit-code sequence. The aperiodic cross-correlation between the code and its mismatched reference is characterized by sidelobes of exactly zero. The compression recovers the 3,000 events without magnitude variations or 'ghost events'.

of incoherent compression in the context of high-resolution B-OCDA is examined below.

B. Incoherent sequence compression in distributed Brillouin sensors

Let us denote the complex envelopes of the Brillouin pump and signal waves, at their respective points of entry into the fiber, as $A_p(t)$ and $A_s(t)$ respectively, where t stands for time. The pump wave enters the fiber at position $z=0$ and propagates in the positive z direction, whereas the signal is launched from the opposite end at $z=L$ and propagates in the negative z direction. The optical frequency of the signal wave is lower than that of the pump by a difference Ω. The fiber under test is characterized by position-dependent profile of the Brillouin frequency shift $\Omega_B(z)$. Typical values of Ω_B in standard fibers at 1550 nm wavelength are $2\pi\cdot 11$ GHz. The linewidth of SBS amplification is $\Gamma_B = 1/\tau$, where $\tau \sim 5$ ns is the acoustic lifetime [1].

Throughout this work the envelopes $A_p(t)$ and $A_s(t)$ are modulated at high rates. The magnitude of the acoustic wave Q that is stimulated at each position z is generally fluctuating in time. One can show that the expectation value of Q, following an initial build-up ($t \gg \tau$), is given by [26]:

$$\overline{Q(\Omega,z)} = jg_1\left[\frac{2\Omega}{\Omega^2{}_B(z)-\Omega-j\Omega\Gamma_B}\right]\gamma_{ps}\left[\Delta(z)\right]. \qquad (1)$$

Here g_1 is an electro-strictive parameter of the fiber,

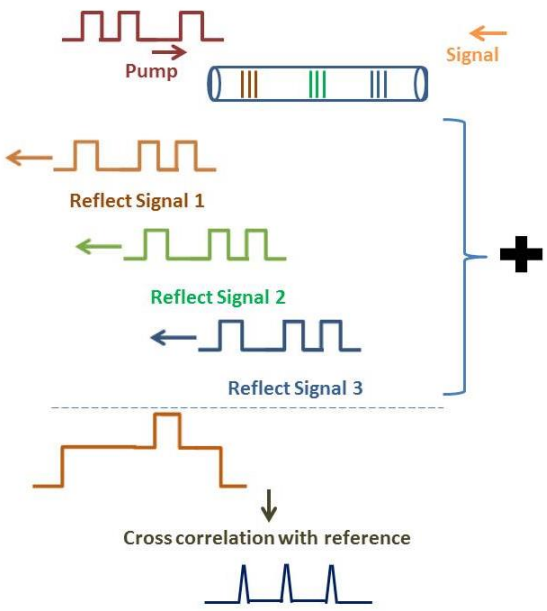

Fig. 3. Application of incoherent sequence compression to phase-coded B-OCDA. The amplitude of the pump wave is coded by a long, aperiodic sequence of comparatively long symbol duration, whereas the amplitude of the signal is fixed. In addition, both waves are phase-modulated by a high-rate, short periodic code (not shown). Phase-coding leads to SBS interactions at discrete, narrow and spatially-periodic correlation peaks. The passing of the pump wave through each peak imprints a replica of its aperiodic amplitude code onto the signal. Overlapping replicas may be separated in post-processing, based on the incoherent compression protocol.

$\Delta(z)=(2z-L)/v_g$ is a position-dependent time lag between pump and signal, v_g is the group velocity of light in the fiber, and $\gamma_{ps}(\Delta)$ denotes the cross-correlation between $A_p(t)$ and $A_s(t)$. The increment in the signal wave power due to the SBS interaction at position z scales with the acoustic field magnitude $|Q|^2$.

Consider first the modulation of both pump and signal by a periodic high-rate, pseudo-random binary phase sequence, with symbol duration $T \ll \tau$ and a period of N symbols. Subject to these boundary conditions, $\overline{Q(\Omega,z)}$ is effectively confined to short segments of width $\Delta z \approx \frac{1}{2}v_g T$ in which $|\gamma_{ps}(\Delta)|^2 = |A_{p0}|^2|A_{s0}|^2$, where $|A_{p0,s0}|$ are the constant magnitudes of pump and signal, respectively [27]. The correlation peaks are separated by a spatial period of $Z = N\cdot\Delta z$ [27]. Between correlation peaks $\overline{Q(\Omega,z)}=0$. The positions of correlation peaks may be scanned with the proper retiming of the phase modulation [27,28].

Suppose next that the pump wave is also modulated by an aperiodic sequence of isolated pulses of duration $\tau < \theta < NT/2$ and equal magnitude $|A_{p0}|^2$, on top of the

periodic phase modulation of both waves. The acoustic field in each correlation peak is stimulated only when a pump pulse reaches its position z. The acoustic field decays at the end of each pulse, until the arrival of the next one. The acoustic field magnitude $Q(\Omega, z)$ at the correlation peak positions is thus switched on and off, following the pattern of pump amplitude modulation, and each stimulation contributes a single amplification event to the magnitude of the signal wave. The SBS interaction at an individual correlation peak position therefore effectively imprints a replica of the aperiodic amplitude modulation sequence onto the signal wave power [10]. The mechanism is schematically illustrated in figure 3.

Since typically $L \gg Z$, a large number of replicas are superimposed on the signal wave, delayed by integer multiples of NT. The magnitude of each replica can be traced back to the strength of SBS in a single correlation peak of known location, which is determined by the timing of underlying phase modulation. However, the echoes of the code are in temporal overlap, and cannot be distinguished directly (see figure 3). The unambiguous analysis of SBS interactions at individual peak locations is analogous to the separation between multiple reflections in an incoherent compression-based radar or range-finder (see figures 1 and 2). We therefore look to employ long, low-PSLR aperiodic sequences in the modulation of the pump wave. Note that the analogue with radar systems in invoked twice in this configuration: first in the generation of correlation peaks through periodic phase-coding, and second in the analysis of multiple peaks via incoherent compression of the aperiodic amplitude sequence.

IV. Numerical simulations

Simulations were required to verify the applicability of incoherent pulse compression principles to high-resolution Brillouin sensors. Although the PSLR performance of long amplitude codes is promising (see figures 1, 2), fundamental differences between radars and B-OCDA must be taken into consideration. The primary concern is the effect of residual Brillouin interactions taking place outside the correlation peaks. While off-peak acoustic waves are weak and their expectation values are zero, their instantaneous magnitudes are nevertheless stochastic with nonzero variance [42]. Residual SBS amplification events outside the intended peak locations accumulate along the entire fiber and contribute an additional noise mechanism, referred to as 'phase coding noise', which is not present in standard radars and not included in the simulations leading to figures 1 and 2.

In attempting to evaluate the prospects of incoherent pulse compression in the context of B-OCDA, the three coupled wave equations for the evolution of the pump, signal and acoustic waves were integrated numerically, subject to the boundary conditions of joint phase and amplitude coding described above:

$$\begin{aligned} A_p(t) &= A_{p0}\sum_n c_{n+n_0} rect\left(\frac{t-nT}{T}\right)\cdot\sum_{m=1}^{M} d_m rect\left(\frac{t-m\theta}{\theta}\right) \\ A_s(t) &= A_{s0}\sum_n c_{n+n_0} rect\left(\frac{t-nT}{T}\right)\cdot \end{aligned} \quad (2)$$

Here $rect(\xi)=1$ when $|\xi|\le 0.5$ and equals zero elsewhere, M = 2,224 is the length of the binary aperiodic amplitude modulation sequence (see section III), $\{d_m\}$ are the elements of amplitude sequence, $\{c_n\}$ denote the elements of a periodic, 255 bits-long phase sequence (the choice of $\{c_n\}$ is discussed below), and n_0 is an arbitrary starting point of the phase sequence at $t=0$. Analysis was performed over fiber lengths up to 3 km. The symbol durations θ and T of the amplitude and phase sequences were 20 ns and 200 ps, respectively.

The length of the simulated fiber was divided into 8 mm-long segments, and the two-way ToF of the optical waves along the fiber was divided in steps of 40 ps [13]. Calculations were carried out in a parallel manner, using a graphics card consisted of 5,000 processing units. Compared with standard personal computer simulations, the duration of calculations was reduced by three orders of magnitude. Even so, the calculation of the signal wave at the output of a 3 km-long fiber, for a single set of correlation peaks positions and for a single value of Ω, required one hour. The simulation of an entire experiment was therefore impractical. Nevertheless, the simulations provide useful insight to the accumulated effect of phase coding noise, which we could not obtain otherwise. All other potential sources of noise were not included in the analysis.

In previous studies, we were able to show that use of so-called *perfect Golomb codes* in periodic phase modulation as part of B-OCDA reduces off-peak interactions considerably, compared with random sequence modulation [42,43]. Ideally, Golomb codes would exhibit off-peak values of their periodic auto-correlation function of exactly zero [44]. However, the perfect correlation is degraded by the exponential window associated with the acoustic wave build-up [45], leading to comparatively large sidelobes at specific Δz offset values. The effective averaging of these residual interactions requires that the starting point n_0 of the Golomb code modulation is varied between successive acquisitions. In experiments, arbitrary offsets are automatically generated since the modulations of amplitude and phase are not synchronized. Variations of n_0 between repeating analyses were included in the simulations as well.

Figure 4(top) shows the simulated, compressed form of the signal wave at the output of a 200 m-long fiber, following averaging over 50 traces. The Brillouin frequency shift in a 7 m-long segment, centered at 275 m distance, was modified by 30 MHz from its value in the rest of the fiber. Calculations were made for $\Omega=\Omega_B$ of the background fiber (blue) and for $\Omega=\Omega_B$ of the modified region (red). A series of compressed impulses is obtained, each representing the SBS amplification in a single correlation peak. The two peaks which are in overlap with the modified fiber segment show a stronger amplification than that of others when Ω matches the Brillouin shift at that region, as expected. The simulation therefore suggests that incoherent compression of the particular code could be applied to phase-coded B-OTDA in 200 m of fiber.

The simulated, compressed trace of the signal wave at the output of a 3 km-long fiber is shown in figure 4(center). Averaging was performed over 95 traces prior to compression. The magnified view of the final 200 m of the fiber, including a 7 m-long modified segment at z = 2,813m, is shown in figure 4(bottom). A series of 600 amplification events can be observed, separated by $z \approx 5$ m as anticipated. However, the magnitudes of the compressed amplification events over the uniform fiber appear uneven, and 'ghost events' appear outside the simulated fiber length. The results are in contrast with those of figure 1(top), where the direct compression of a similar number of echoes of the same sequence provided an impulse series that was much more uniform. In addition, the difference between the two peaks which are in overlap with the modified segment and all other events is smaller than in panel 4(top).

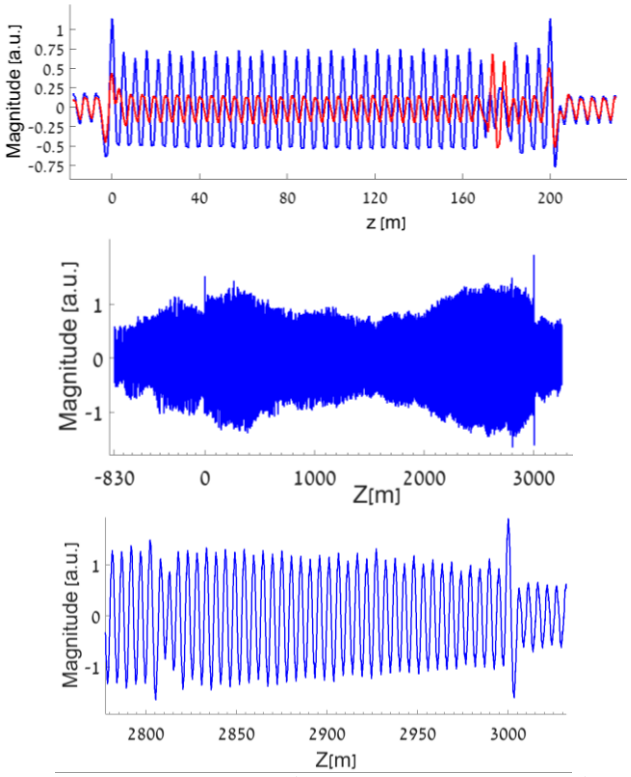

Fig. 4. Top - Simulated SBS amplification at 40 correlation peaks of 2 cm-width, along a 200 m-long fiber. The pump wave was amplitude-modulated by an aperiodic binary sequence of 2,224 symbols, with bit duration of 20 ns. Both pump and signal were phase-modulated by a periodic 255 bit-long Golomb code, with symbol duration of 200 ps. The output signal wave was calculated through the numerical integration of the coupled differential equations for pump, signal and acoustic waves. The output trace was averaged over 50 realizations and compressed through cross-correlation with a mismatched filter, designed to minimize the sidelobes of the aperiodic amplitude code. The Brillouin frequency shift was offset by 30 MHz within a 7 m-long segment, at z = 275 m. Blue (red) trace corresponds to a difference Ω between the frequencies of pump and signal that matches the Brillouin shift outside (within) the modified region. 40 distinct and uniform compressed events may be seen in both traces. The two peaks which are in overlap with the modified region are less pronounced than all others in the blue trace, and stronger than the rest in the red trace, as expected.

Center - Simulated SBS amplification at 600 correlation peaks along a 3 km-long fiber, using the same parameters as above and averaged over 95 traces. Uneven magnitudes of compressed events, and 'ghost peaks' at z < 0 m and z > 3,000 m are apparent.

Bottom - Magnified view of the final 200 m of the fiber of the central panel simulation. The Brillouin frequency shift was offset by 30 MHz within a 7 m-long segment, at z = 2813 m. The two compressed impulses which correspond to peaks within the modified segment are lower than adjacent events. The difference, however, is much less pronounced than in the simulation of a shorted fiber in the top panel.

The difference between figures 1 and 3 is due to the detrimental effect of phase coding noise. The compression of the 2,224 bit-long amplitude sequence might not be efficient enough for the precise, simultaneous analysis of SBS gain spectra in hundreds of resolution points, and a longer, better code might be necessary. The experiments reported below therefore make use of the 9,785 bit-long sequence of figure 2(bottom). The numerical simulation of B-OCDA with aperiodic amplitude modulation using that sequence is extremely involved, and is still under study.

V. Experimental Setup and Results

The experimental setup used in high-resolution Brillouin analysis with a large number of addressed points is shown schematically in figure 5. Light from a laser diode source at 1550 nm wavelength passed through an electro-optic (EO) phase modulator, driven by the output voltage of an arbitrary waveform generator (AWG). The AWG was programmed to repeatedly generate a 211 bits-long Golomb code with T of 200 ps (Δz of 2 cm). The voltage magnitude of the AWG was adjusted to match V_π of the EO modulator.

The modulated signal was split into two branches. Light at the pump branch passed through a single-sideband EO modulator, driven by a radio frequency (RF) sine wave of frequency $\Omega \approx \Omega_B$. The pump was then amplitude-modulated by an aperiodic 9,785 bits-long binary sequence (see section III) using another AWG, with θ of 20 ns. Lastly, the pump wave was amplified to an average power level of 150 mW by an EDFA and launched into an 8.8 km-long fiber under test (FUT).

At the signal branch, a 60 km-long fiber delay was used to allow for the scanning of the correlation peaks positions ([28], see below). A polarization scrambler was used to avoid polarization-induced fading of the SBS interactions [46]. The signal was then launched into the opposite end of the FUT. The output signal was detected by a 200 MHz-wide photo-detector, and the detector output was sampled by a digitizing oscilloscope and averaged over N_{av} = 256 repetitions. Each averaged trace was cross-correlated with a carefully constructed reference sequence, using offline digital processing [12,36]. As many as 2,100 correlation peaks were simultaneously addressed in each trace.

The pump and signal branches of the setup and the FUT formed a long fiber loop. The middle of the loop is located at equal distances from the splitting point at the phase modulator output (see figure 5), in the clockwise and counter-clockwise directions. The middle of the loop is located within the fiber imbalance path. A large number of correlation peaks were established along the loop. An individual correlation peak of order m, with m a positive or negative integer, was located at a distance $Z_m = \frac{1}{2} mNv_g T$ from the middle of the loop. The positions of all nonzero-order peaks could therefore be moved

This article has been accepted for publication in a future issue of this journal, but has not been fully edited. Content may change prior to final publication. Citation information: DOI 10.1109/JLT.2016.2521173, Journal of Lightwave Technology

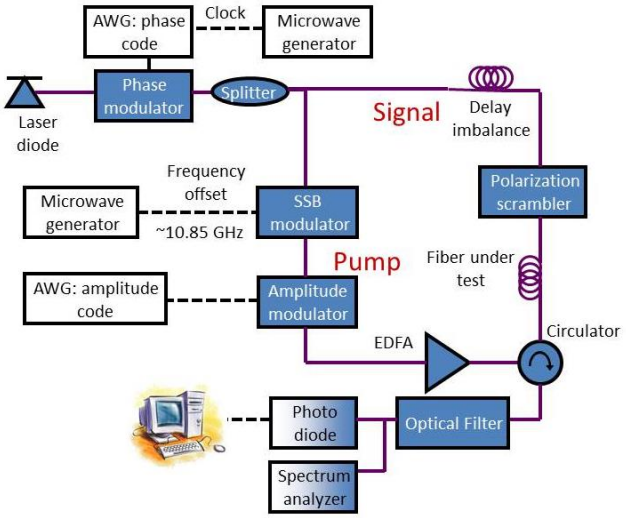

Fig. 5. Experimental setup for long-reach, high-resolution distributed Brillouin fiber analysis. SSB: single sideband. AWG: arbitrary waveform generator. EDFA: erbium-doped fiber amplifier. Solid lines denote fiber path, and dashed lines represent radio-frequency electrical cables.

by slight changes ΔT to the symbol duration: $\Delta Z_m / Z_m = \Delta T / T$ [28].

Let us denote the highest (lowest) order of correlation peaks that were in overlap with the FUT as $m_{\max}(m_{\min})$. A sufficiently long delay imbalance in the signal path guaranteed that $(m_{\max} - m_{\min}) \ll m_{\min}$. Consequently, the positions of all correlation peaks could be scanned with practically equal increments, which were set to match the resolution step: $\Delta Z_m \approx \Delta z$, for all $m_{\min} < m < m_{\max}$. The long fiber delay allowed for the rapid, all-electrical scanning of correlation peak positions, with no moving parts and over long ranges [28].

In each positioning step, the output signal was recorded for 34 frequency offsets Ω, in step increments δ of 3 MHz. Following N position steps $\{Z_{m-1}\}$ reached the initial locations of $\{Z_m\}$, and the data acquisition was complete. The overall duration of the experiment was several hours, limited by the switching times of multi-purpose laboratory equipment.

Figure 6(top) shows a map of the Brillouin gain as a function of Ω and z [13]. The analysis of all 440,000 resolution points is presented. Figure 6(bottom) shows a magnified view of the gain map in the vicinity of a 7 cm-long hot-spot, located towards the output end of the pump wave. The hot-spot is properly recognized in the measurements. The setup is capable of resolving shorter events, on the order of Δz, however this limit was not reached in the experiment. The experimental uncertainty σ_ν in $\Omega_B(z)$, estimated by the standard deviation of the local difference $\left[\Omega_B(z+\Delta z) - \Omega_B(z)\right]/(2\pi)$, was ±3.5 MHz.

VI. Discussion

In this work, we reported a distributed Brillouin sensor experiment over 8.8 km of fiber with a 2 cm resolution. The entire set of 440,000 potential resolution points was addressed.

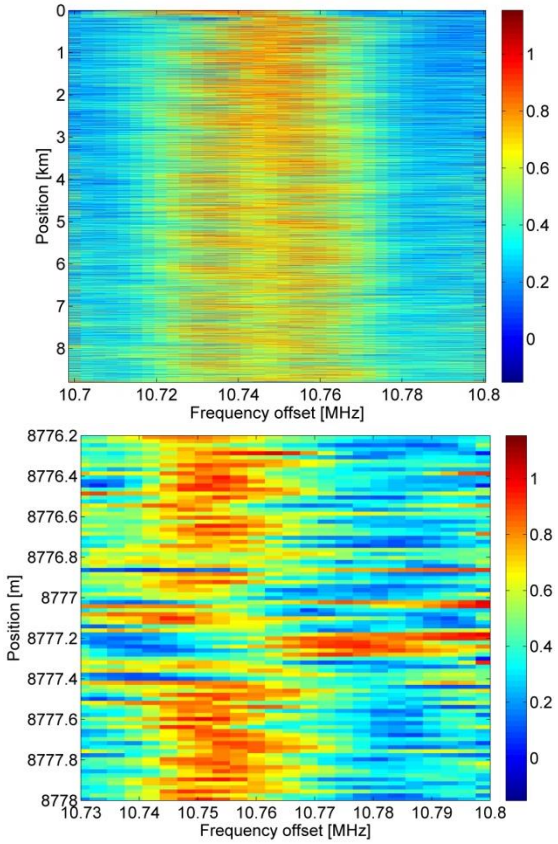

Fig. 6. Top - Measured Brillouin gain of the output signal wave (in arbitrary units), as a function of correlation peak position, and of the frequency difference between pump and signal waves. 440,000 resolution points are addressed. Bottom - Magnified view of the gain map in the vicinity of a 7 cm-long hot spot, located towards the output end of the pump wave [13].

The number of points is four times larger than that of our previous experiments [10]. While the previous results provided proof of the proposed concept, the current work was meant to reach considerably longer range and larger number of points.

The measurement was based on the dual-hierarchy modulation of the optical waves. Both pump and signal were jointly phase-modulated by a periodic, high-rate binary phase sequence. The amplitude of the pump wave was also amplitude-modulated by a lower-rate, aperiodic, long sequence, chosen for its theoretically perfect cross-correlation with a carefully constructed mismatched reference. The measurement principle is inspired by the analogy between distributed fiber sensors and radar systems.

The limitations of the measurement protocol were examined in large-scale numerical simulations of SBS over km of fiber with sub-cm resolution, using the proposed modulation scheme as the boundary condition. Calculations were carried out in parallel over 5,000 graphics processing units. The simulations results highlight the fundamental differences between the mathematically perfect correlation properties of the codes involved, and their physical representation in SBS. The detrimental effect of residual off-peak interactions is illustrated.

A figure of merit for the performance of Brillouin distributed sensors was proposed by Soto and Thevenaz in 2013 [47]:

$$FoM = \frac{\left(\alpha L_{eff}\right)^2 e^{2\alpha L}}{\Delta z\sqrt{N_{av}N_{phase}}}\frac{\sqrt{\delta\cdot\left(\Gamma_B/2\pi\right)}}{\sigma_v}. \quad (3)$$

Here α is the loss coefficient of the fiber under test, and L_{eff} is its effective length. In our experiments the duration of the entire amplitude sequence is longer than the ToF along the FUT, by a factor of 4.6. The value of N_{av} used in Eq. (3) is increased accordingly, to account for the duration of data acquisition. The figure of merit of the current experiment is 0.08 m^{-1}. It is 8 times better than that of our previous work [10]. Progress with respect to our previous work was enabled primarily by the introduction of a longer, improved amplitude modulation sequence. Yet, the figure of merit is still short of the best reported values of high-resolution B-OTDA setups (0.2 m^{-1} for the system described in [20]).

It should be noted that the figure of merit does not acknowledge the number of resolution points that are actually addressed in a given experiment. Addressing very large sets of points is one of the primary challenges in high-resolution B-OCDA. To the best of our knowledge, while setups with a larger number of potential resolution points were previously proposed [32,33], the current results represent the largest set of resolution points actually addressed in any SBS-based sensor to-date.

The main drawback of the system described in this work, and of B-OCDA in general, is the large number N of correlation peak position scans that is necessary to reconstruct the gain spectra along the entire fiber (211 scans in our case). In contrast, double-pulse B-OTDA setups only require 2 scans. On the other hand, the system presented here has the advantages of longer range, and potentially reduced number of averages N_{av} due to narrowband detection. The latter, however, was not fully exploited at the current experiment, since the number of averages was also restricted by the operation rate of the polarization scrambler. Future work would make use of polarization switching instead, as recently proposed in [48,49]. The necessary number of averages, without polarization scrambling, will be determined by phase coding noise as illustrated in simulations. It is expected that fewer averages than the 256 used here would be sufficient in that case, however further work is needed to establish the lower limit.

The merit of Brillouin radar-like analysis would become more significant with increasing distance, due to depletion consideration. A B-OTDA pulse experiences depletion along the entire length of the fiber, while the interaction of B-OCDA pump pulses with the signal wave is inefficient outside correlation peaks. The high-rate phase modulation of the B-OCDA pump also suppresses spontaneous Brillouin scattering. We therefore anticipate that analysis protocol presented here might scale better to the analysis of very large numbers of high-resolution points.

In conclusion, a state-of-the-art, high-resolution distributed Brillouin sensor demonstration has been achieved. Ongoing work is being dedicated to the employment of advanced sensing protocols to the monitoring of transportation infrastructure and composite materials [50], to numerical simulations using the long amplitude sequence used in the experiments, and to reducing the necessary number of averages and acquisition times. And lastly, the dramatic SNR improvement of B-OTDA, demonstrated recently using image-processing of the SBS gain map [51], is applicable to the post-processing of data collected using the protocol described in this work as well.

REFERENCES

[1] R. W. Boyd *Nonlinear Optics*, 3rd Edition. Academic Press, 2008.

[2] T. Kurashima, T. Horiguchi, and M. Tateda, 1990 "Distributed-temperature sensing using stimulated Brillouin scattering in optical silica fibers," *Opt. Lett*. vol. 15, no. 18, pp. 1038-40, Sep. 1990.

[3] M. Niklès, L. Thévenaz, and P. A. Robert, "Simple distributed fiber sensor based on Brillouin gain spectrum analysis," *Opt. Lett*., vol. 21, no. 10, pp. 758-760, May 1996.

[4] F. Gyger, E. Rocha, S. Chin, M. Niklès, and L. Thévenaz, "Extending the sensing range of Brillouin optical time-domain analysis up to 325 km combining four optical repeaters," *Proc. of 23rd Optical Fiber Sensors Conference (OFS-23), (Santander, Spain, 2-6 June 2014),* Proc. SPIE, vol. 9157, 91576Q, 2014.

[5] Y. Peled, A. Motil, and M. Tur, "Fast Brillouin optical time domain analysis for dynamic sensing," *Opt. Express*, vol. 20, no. 8, pp. 8584-8591, Apr. 2012.

[6] Y. Peled, A. Motil, I. Kressel, and M. Tur, "Monitoring the propagation of mechanical waves using an optical fiber distributed and dynamic strain sensor based on BOTDA," *Opt. Express*, vol. 21, no. 9, pp. 10697-10705, May 2013.

[7] J. Urricelqui, A. Zornoza, M. Sagues, and A. Loayssa, "Dynamic BOTDA measurements based on Brillouin phase-shift and RF demodulation," *Opt. Express*, vol. 20, no. 24, pp. 26942-26949, Nov. 2012.

[8] I. Sovran, A. Motil, and M. Tur, "Frequency-scanning BOTDA with ultimately fast acquisition speed," *IEEE Photon. Technol. Lett.*, vol. 27, no. 13, pp. 1426-1429, Jul. 2015.

[9] A. Minardo, A. Coscetta, S. Pirozzi, R. Bernini, and L. Zeni, "Modal analysis of a cantilever beam by use of Brillouin based distributed dynamic strain measurements," *Smart Materials and Structures*, vol. 21, 125022, Nov. 2012.

[10] Y. London, Y. Antman, R. Cohen, N. Kimelfeld, N. Levanon, and A. Zadok, "High-resolution long-range distributed Brillouin analysis using dual-layer phase and amplitude coding," *Opt. Express*, vol. 22, no. 22, pp. 27144-27158, Nov. 2014.

[11] N. Levanon, "Noncoherent pulse compression," *IEEE T. Aero. Elec. Sys.*, vol. 42, no. 2, pp. 756–765, Apr. 2006.

[12] N. Levanon, I. Cohen, N. Arbel, and A. Zadok, "Non-coherent pulse compression – aperiodic and periodic waveforms," *IET Radar Sonar and Navigation*, vol. 9, accepted for publication (in press), 2015.

[13] Y. London, Y. Antman, N. Levanon, and A. Zadok, "Brillouin analysis with 8.8 km range and 2 cm resolution," *Proc. of 24th Optical Fiber Sensors Conference (OFS-24), (Curitiba, Brazil, 28 September – 2 October 2015)* Proc. SPIE, vol. 9364, 96340G, 2015.

[14] A. Fellay, L. Thévenaz, M. Facchini, M. Nikles, and P. A. Robert, "Distributed sensing using stimulated Brillouin scattering: towards ultimate resolution," *Proc. of 12th Optical Fiber Sensors Conference (OFS-12)* (Williamsburg VA, October 28, 1997), Proc. Optical Society of America, OWD3, 1997.

[15] J. C. Beugnot, M. Tur, S. Foaleng Mafang, and L. Thévenaz, "Distributed Brillouin sensing with sub-meter spatial resolution: modeling and processing," *Opt. Express*, vol. 19, no. 8, pp. 7381-7397, Apr. 2011.

[16] X. Bao and L. A. Chen, "Recent progress in Brillouin scattering based fiber sensors," *Sensors*, vol. 11, no. 4, pp. 4152-4187, Apr. 2011.

[17] V. Lecoeuche, D. J. Webb, C. N. Pannell, and D. A. Jackson, "Transient response in high-resolution Brillouin based distributed sensing using probe pulses shorter than the acoustic relaxation time," *Opt. Letters*, vol. 25, no. 3, pp. 156–158, Feb. 2000.

[18] F. Wang, X. Bao, L. Chen, Y. Li, J. Snoddy, and X. Zhang, "Using pulse with dark base to achieve high spatial and frequency resolution for the distributed Brillouin sensor," *Opt. Letters*, vol. 33, no. 22, pp. 2707-2709, Nov. 2008.

[19] A. W. Brown, B. G. Colpitts, and K. Brown, "Distributed sensor based on dark-pulse Brillouin scattering," *IEEE Photon. Technol. Lett*., vol. 17, no. 7, pp. 1501-1503, Jul. 2005.

[20] S. Foaleng Mafang, M. Tur, J. C. Beugnot, and L. Thevenaz, "High spatial and spectral resolution long-range sensing using Brillouin echoes," *J. Lightwave Technol*., vol. 28, no. 20, pp. 2993-3003, Oct. 2010.

[21] W. Li, X. Bao, Y. Li, and L. Chen, "Differential pulse-width pair BOTDA for high spatial resolution sensing," *Opt. Express*, vol. 16, no. 26, pp. 21616-21625, Dec. 2008.

[22] Y. Dong, H. Zhang, L. Chen, and X. Bao, "2 cm spatial-resolution and 2 km range Brillouin optical fiber sensor using a transient differential pulse pair," *Appl. Optics*, vol. 51, no. 9, pp. 1229-1235, Mar. 2012.

[23] K. Hotate and T. Hasegawa "Measurement of Brillouin gain spectrum distribution along an optical fiber using a correlation-based technique-proposal, experiment and simulation," *IEICE T. Electron*., vol. E83-C, no. 3, pp. 405–412, Mar. 2000.

[24] O. Matsuoka, M. Kishi, and K. Hotate, "Brillouin optical correlation domain reflectometry with double frequency modulation and phase modulation," *Proc. of 23rd Optical Fiber Sensors Conference (OFS-23), (Santander, Spain, 2-6 June 2014)*, Proc. SPIE, vol. 9157, 91576G, 2014.

[25] K. Y. Song, Z. He, and K. Hotate, "Distributed strain measurement with millimeter-order spatial resolution based on Brillouin optical correlation domain analysis," *Opt. Lett*., vol. 31, no. 17, pp. 2526-2528, Sep. 2006.

[26] R. Cohen, Y. London, Y. Antman, and A. Zadok, "Brillouin optical correlation domain analysis with 4 millimeter resolution based on amplified spontaneous emission," *Opt. Express*, vol. 22, no. 10, pp. 12070-12078, May 2014.

[27] Y. Antman, N. Primerov, J. Sancho, L. Thévenaz, and A. Zadok, "Localized and stationary dynamic gratings via stimulated Brillouin scattering with phase modulated pumps," *Opt. Express*, vol. 20, no. 7, pp. 7807-7821, Mar. 2012.

[28] A. Zadok, Y. Antman, N. Primerov, A. Denisov, J. Sancho, and L. Thévenaz, "Random-access distributed fiber sensing," *Laser Photonics Rev*., vol. 6, no. 5, pp. L1-L5, 2012.

[29] A. Denisov, M. A. Soto, and L. Thévenaz, "Time gated phase-correlation distributed Brillouin fiber sensor," *Proc. Fifth European Workshop on Optical Fiber Sensors, (Krakow, Poland, 2014)*, Proc. SPIE, vol. 8794, 87943I, 2014.

[30] D. Elooz, Y. Antman, N. Levanon, and A. Zadok, "High-resolution long-reach distributed Brillouin sensing based on combined time-domain and correlation-domain analysis," *Opt. Express*, vol. 22, no. 6, pp. 6453-6463, Mar. 2014.

[31] D. Elooz, Y. Antman, and A. Zadok, "Combined time-domain and correlation-domain Brillouin analysis with 1600 meters range and 2 centimeters resolution," *Proc. of 23rd Optical Fiber Sensors Conference (OFS-23), (Santander, Spain, 2-6 June 2014)*, Proc. SPIE, vol. 9157, 91576O, 2014.

[32] A. Denisov, M. A. Soto, and L. Thévenaz, "1'000'000 resolved points along a Brillouin distributed fiber sensor," *Proc. of 23rd Optical Fiber Sensors Conference (OFS-23), (Santander, Spain, 2-6 June 2014)*, Proc. SPIE, vol. 9157, 9157D2, 2014.

[33] K. Y. Song, Y. H. Kim, and K. Lee, "Brillouin optical correlation domain analysis with more than 1 million effective sensing points," *Proc. of 24th Optical Fiber Sensors Conference (OFS-24), (Curitiba, Brazil, 28 September – 2 October 2015)*, Proc. SPIE, vol. 9634, 96340I, 2015.

[34] N. Levenon and E. Mozeson, *Radar Signals*, New York, NY: Wiley, 2004.

[35] X. Angulo Vinuesa, A. Lopez Gil, A. Dominguez López, J. L. Cruz, M. V. Andres, S. Martin Lopez, and M. Gonzalez-Herraez, "Simultaneous gain and phase profile determination on an interferometric BOTDA," *Proc. of 24th Optical Fiber Sensors Conference (OFS-24), (Curitiba, Brazil, 28 September – 2 October 2015)*, Proc. SPIE, vol. 9634, 963419, 2015.

[36] D. Kravitz, D. Grodensky, N. Levanon, and A. Zadok, "High-resolution low-sidelobe laser ranging based on incoherent pulse compression," *IEEE Photonic Tech. Lett*., vol. 24, no. 23, pp. 2119-2121, Dec. 2012.

[37] A. Ilovitsh, E. Preter, N. Levanon, and Z. Zalevsky, "Time multiplexing super resolution using a Barker-based array," *Opt. Letters*, vol. 40, no. 2, pp. 163-165, Jan. 2015.

[38] M. A. Soto, G. Bolognini, F. Di Pasquale, and L. Thévenaz, "Simplex-coded BOTDA fiber sensor with 1 m spatial resolution over a 50 km range," *Opt. Letters*, vol. 35, no. 2, pp. 259-261, Jan. 2010.

[39] M. A. Soto, X. Angulo-Vinuesa, S. Martin-Lopez, S. Chin, J. D. Ania-Castanon, P. Corredera, E. Rochat, M. Gonzalez-Herraez, and L. Thevenaz, "Extending the real remoteness of long-range Brillouin optical time domain fiber analyzers," *J. Lightwave Technol*., vol. 32, no. 1, 152-162, Jan. 2014.

[40] M. A. Soto, G. Bolognini, F. Di Pasquale, and L. Thévenaz, "Long-range Brillouin optical time-domain analysis sensor employing pulse coding techniques," *Meas. Sci. Technol*., vol. 21, 094024, Jul. 2010.

[41] M. A. Soto, S. Le Floch, and L. Thévenaz, "Bipolar optical pulse coding for performance enhancement in BOTDA sensors," *Opt. Express*, vol. 21, no. 14, pp. 16390–16397, Jul. 2013.

[42] Y. Antman, N. Levanon, and A. Zadok, "Low-noise delays from dynamic Brillouin gratings based on perfect Golomb coding of pump waves," *Opt. Lett*., vol. 37, no. 24, pp. 5259-5261, Dec. 2012.

[43] Y. Antman, L. Yaron, T. Langer, M. Tur, N. Levanon, and A. Zadok, "Experimental demonstration of localized Brillouin gratings with low off-peak reflectivity established by perfect Golomb codes," *Opt. Lett*., vol. 38, no. 22, pp. 4701-4704, Nov. 2013.

[44] S. W. Golomb, "Two-valued sequences with perfect periodic autocorrelation," *IEEE T. Aero. Elec. Sys.*, vol. 28, no. 2, pp. 383-386, Apr. 1992.

[45] Y. Antman, L. Yaron, T. Langer, M. Tur, and A. Zadok, "Variable delay of Gbit/s data using coded Brillouin dynamic gratings," *Proc. Photonics West Conference (San Francisco CA, February 2014)*, Proc. SPIE, vol. 8998, Advances in Slow and Fast Light VII, 89980W, 2014.

[46] A. Zadok, E. Zilka, A. Eyal, L. Thevenaz, and M. Tur, "Vector analysis of stimulated Brillouin scattering amplification in standard single-mode fibers," *Opt. Express*, vol. 16, pp. no. 26, 21692-21707, Dec. 2008.

[47] M. A. Soto and L. Thévenaz, "Modeling and evaluating the performance of Brillouin distributed optical fiber sensors," *Opt. Express*, vol. 21, no. 25, pp. 31347-31366, Dec. 2013.

[48] J. Urricelqui, F. Lopez-Fernandino, M. Sagues, and A. Loayssa, "Polarization diversity scheme for BOTDA sensors based on a double orthogonal pump interaction," *IEEE J. Lightwave Technology*, vol. 33, no. 12, pp. 2633-2638, Jun. 2015.

[49] A. López-Gil, A. Domínguez-López, S. Martín-López and M. González-Herráez, "Simple method for the elimination of polarization noise in BOTDA using balanced detection of orthogonally polarized Stokes and anti-Stokes probe sidebands," *Proc. of 23rd Optical Fiber Sensors Conference (OFS-23), (Santander, Spain, 2-6 June 2014)*, Proc. SPIE, vol. 9157, 91573U, 2014.

[50] Y. London, Y. Antman, M. Silbiger, L. Efraim, A. Froochzad, G. Adler, E. Levenberg, and A. Zadok, "High-resolution Brillouin analysis of composite materials beams," *Proc. of 24th Optical Fiber Sensors Conference (OFS-24), (Curitiba, Brazil, 28 September – 2 October 2015)*, Proc. SPIE, vol. 9634, 96346N, 2015.

[51] M. A. Soto, J. A. Ramirez, and A. Thevenaz, "Intensifying Brillouin distributed fiber sensors using image processing," *Proc. of 24th Optical Fiber Sensors Conference (OFS-24), (Curitiba, Brazil, 28 September – 2 October 2015)*, Proc. SPIE, vol. 9634, 96342D, 2015.